Self-Limiting Heterogeneous Reactions: Bifunctional Hydrocarbon on a Bimetallic Alloy Surface

Hong He, Anna T. Mathauser, and Andrew V. Teplyakov*

Department of Chemistry and Biochemistry, University of Delaware, Newark, Delaware 19716

Received: July 26, 2000; In Final Form: September 26, 2000

Here we report the remarkable chemistry exhibited by 6-bromo-1-hexene on a $Cu_3Pt(111)$ surface. The dehydrocyclization reaction leading to the formation of benzene takes place at very low coverage; as the surface fills up, decomposition becomes a predominant pathway. Further increase of the surface concentration of 6-bromo-1-hexene leads to the hydrogenation of 5-hexenyl formed on a surface as a result of C−Br bond dissociation. This reaction produces 1-hexene, which is stable on the surface until the molecular desorption of this compound commences at 230 K. Molecular desorption of 6-bromo-1-hexene from the monolayer becomes significant at even higher exposures. All these processes occur very cleanly within a specific coverage range, making the 6-bromo-1-hexene on the $Cu_3Pt(111)$ surface extremely attractive for analysis of kinetics of coverage-dependent reactions. Steric requirements for each of the processes described here and the availability of the adsorption sites on the alloy surface are believed to govern the predominant reaction.

Introduction

Chemical transformation of linear hydrocarbons has always been the focus of various industrial applications. Heterogeneous catalysis of hydrocarbon derivatives is implemented in petroleum refinement, selective synthesis of chemicals, disposal of harmful wastes, and in many other fields. The transition metals have received significant attention as they showed the most controllable catalytic properties and were usually the basis of industrial catalysts for the chemical processes involving hydrocarbon derivatives. Single-crystal studies (see, for example, refs 1−14 and references therein) and the research on supported metal catalysts prepared in a controlled manner[12,15] have been the source of the most reliable mechanistic and thermodynamic information about all these processes since ultrahigh vacuum surface analytical techniques became available. This information was extremely valuable in understanding the basic thermodynamics and kinetics of surface reactions and the geometrical requirements for a variety of chemical processes.

In the single-crystal studies of transition metals, the processes occurring at low coverages have usually been the focus of research because at these conditions single steps of each process could be easily isolated and investigated.[7−9] At the same time, the concern has grown that these mechanistic studies may not always be related to the industrial high-pressure and high-temperature transformations. Unfortunately, at this point the *mechanistic* studies of the hydrocarbon conversion under real conditions are relatively scarce because of the limitations of the techniques that can be used and because of the complicated chemical reactions competing at these conditions. Thus, ultrahigh vacuum studies at high coverages may provide vital information for relating single-crystal work and industrial requirements.

The specific system considered here is 6-bromo-1-hexene on a $Cu_3Pt(111)$ surface. Cu_3Pt has been shown to possess interesting catalytic properties and the choice of this alloy can be rationalized by the cumulative properties of copper and platinum.

Platinum in the form of a single crystal has been the subject of numerous studies. This noble metal is used in catalytic processes involving C−C or C−H bond formation or scission. It shows a very high reactivity and its selectivity can be altered by tuning the process conditions. In industrial applications platinum is usually used on a support because of the extremely high price of this metal. The catalytic properties of platinum often vary as a function of the support material, and the studies of this effect constitute a separate research area.

On the other hand, pure copper is rarely used as a hydrogenation/dehydrogenation catalyst; however, its high reactivity toward carbon−halogen bond scission has led to the uses of this transition metal as a catalyst for halogenated waste regeneration. Thus, copper−platinum alloy may exhibit an attractive set of catalytic properties. It would be too simplistic to model the collective properties of an alloy by analyzing the chemical properties of its pure components, but as will be shown below, copper−platinum system supports these speculations to a significant extent.

The detailed chemical studies of single crystals of bimetallic alloys have been slowed by the fact that these single crystals are difficult to obtain. Instead, surface alloys have often been the subject of the research in this field. Sn/Pt(111),[16−18] Au/Pt(100),[19,20] Au/Pt(111),[21] Pt/Au(100),[19,20] Sn/Pt(111),[16−18,22] and Bi/Pt(111)[23−27] surfaces were studied as dehydrogenation catalysts and it was shown that alloying of platinum with other metals increases the rate of dehydrogenation and decreases the percentage of decomposition. This research advanced greatly the understanding of C−H bond interaction with platinum.

The catalytic properties of noble metals have been shown to change significantly upon alloying with other metals,[28−33] and the explanation for such behavior is needed. Besides the changes in electronic properties of metals upon alloying, the possible causes for such an altered reactivity would be variations in the geometric arrangement of the catalytic sites,[29] bonding energy

* Corresponding author: fax (302) 831-6335; e-mail andrewt@udel.edu.

10.1021/jp0026787 CCC: $19.00
Published on Web 12/01/2000

of reactants or products,[21,34] or suppression of possible competing surface processes.[31,34,35]

In the late 1970s de Jongste et al. showed that copper−platinum alloys are excellent catalysts for aromatization reaction[36] and that their reactivity can be altered by changing the concentration of the metals.[37−39] Dechlorination reactions have recently been studied on Cu−Pt alloys supported on activated carbon.[40] Detailed molecular level mechanistic studies of some of these alloys have only been performed very recently as several single-crystal alloys became available. The most characterized among these alloys is Cu_3Pt.[41−49] Theoretical studies by Hammer and Nørskov[50] investigated the (111) surface of this alloy and suggested that the electronic properties of platinum and copper atoms on this surface are much more similar to each other than to the properties of pure platinum and pure copper, respectively. At the same time, the density of states with respect to the Fermi level on the $Cu_3Pt(111)$ surface is shown to be shifted to the average position between pure platinum and pure copper.[50] Thus, the potential for tuning the physical properties of copper−platinum alloys has been established. Density of electronic states is only one of the factors that affect the catalytic properties of metals or alloys; however, in many catalytic reactions electron transfer is the major step and catalytic reactivity will depend directly on the electronic properties of the surface.

Several ultrahigh vacuum studies of $Cu_3Pt(111)$ have been reported. Adsorption of Xe,[51] H_2,[52−55] CO,[54−60] and unsaturated hydrocarbons and aromatization of linear and cyclic hydrocarbons[61,62] have been investigated in detail at low coverages. High-coverage studies of chemical transformations of multifunctional organic compounds on this surface promise to be quite interesting because of a wide range of surface reactivity with respect to different chemical groups.

Studies presented in this paper combine the temperature-programmed reaction/desorption (TPR/D) and Auger electron spectroscopy (AES) investigation of 6-bromo-1-hexene on a $Cu_3Pt(111)$ surface with near-edge X-ray absorption fine structure (NEXAFS) studies. The experimental evidence suggests that this system exhibits two different coverage regimes before the multilayer desorption commences. The division of all surface chemical reactions into two categories, low coverage and high coverage, is quite vague. Often high coverage is associated with the presence of the multilayer, but sometimes it is related to the presence of multiple species crowding the single-crystal surface.[63,64] On the basis of the NEXAFS measurements, these regimes were identified here as a *low-coverage regime* that corresponds to 6-bromo-1-hexene adsorbed with the alkyl chain approximately parallel to the surface and a *high-coverage regime* that corresponds to practically random distribution of the alkyl chains of the 6-bromo-1-hexene molecule within the monolayer. At low concentration of surface species, two chemical processes were shown to occur after C−Br dissociation. When there is enough space on the surface for 5-hexenyl (the product of C−Br dissociation) to rearrange, the only process following the thermal annealing is the formation of benzene. This process has been analyzed in detail for 1-hexene on $Cu_3Pt(111)$.[61,62] After 1.5 Langmuir limit is reached, decomposition is the only other pathway besides benzene formation up until the exposure is raised to 3 Langmuirs. At this point the majority of the surface is covered with 6-bromo-1-hexene lying flat. The surface regions that are still available for adsorption are too small to accommodate an entire 6-bromo-1-hexene molecule. Upon further increase of the exposure of 6-bromo-1-hexene, the formation of 1-hexene by hydrogenation of 5-hexenyl becomes predominant. Finally, at even higher exposures, molecular desorption of 6-bromo-1-hexene from the monolayer is the main pathway. Only after the initial dose of 6-bromo-1-hexene reaches 8.5 Langmuirs does molecular desorption from the multilayer commence. Self-governing mechanisms of these chemical transformations seem to be determined by the geometrically restricted structure[65] of the monolayer. Known structures with restricted geometries include micelles and vesicular systems,[65−68] polymer solutions,[69] zeolites,[70] porous glasses,[71] silica gels,[72] and nanoparticles;[65] however, here we report a self-organized structure evolved on a single-crystal alloy surface as a result of its own submonolayer chemical transformations.

Experimental Section

The experimental studies presented here were performed on two ultrahigh vacuum (UHV) chambers. The instrument at the University of Delaware that was used for thermal desorption studies has a background pressure of 3×10^{-10} Torr. It is equipped with an Auger electron spectrometer (AES), an apparatus for low-energy electron diffraction (LEED), an ion gun for surface sputtering, and a shielded quadrupole mass spectrometer (Stanford Research Systems) differentially pumped by the chamber. In the temperature-programmed desorption studies the adsorbate-covered surface was positioned in line-of-sight with the mass spectrometer, approximately 3 mm from a 4 mm diameter sampling aperture. This arrangement allows for accurate detection of the molecules desorbing from the center of the single-crystal surface.

The NEXAFS measurements were conducted on beamline U1A of the National Synchrotron Light Source at Brookhaven National Laboratory. A detailed description of the experimental end station has been given elsewhere.[73] This UHV chamber has a background pressure of 5×10^{-10} Torr. It is equipped with an Auger electron spectrometer, mass spectrometer, and ion gun for surface cleaning. The NEXAFS spectra were recorded with a partial electron yield detector with a retarding voltage of −150 V. The resolution of the synchrotron monochromator was set to approximately 0.7 eV near the C K-edge region.

Each NEXAFS spectrum was divided by the signal from a reference grid that measures the intensity of the incident beam simultaneously with the NEXAFS spectra. This resulting spectrum is then divided by the same ratio collected for the clean sample surface. The validity of such treatment has been discussed in detail previously.[74]

The $Cu_3Pt(111)$ single crystal was obtained from Material Technologie & Kristalle Gmbh (Jülich, Germany) as a circular disk of 1 cm diameter and 2 mm in thickness polished to a mirror finish on one (111) surface. The crystal was mounted to a resistive heating element and attached to a manipulator with capabilities of heating the surface to 1000 K and cooling it to 120 K with liquid nitrogen. The temperature of the crystal was measured by a chromel−alumel thermocouple wedged into a hole on a side of the crystal. A temperature ramp of 2 K/s was maintained for all the thermal desorption studies presented here by a temperature programmer (Eurotherm 818 P) connected to a dc power supply (Hewlett-Packard 6291A). The alloy crystal was prepared by Ar^+ sputtering at 550 K for 15 min followed by annealing in UHV at 840 K for 20 min.[57] The cleanliness of the surface after this procedure was confirmed by AES. A (1 × 1) diffraction pattern was observed by LEED.[52,54,55,75,76]

6-Bromo-1-hexene (98%, Alfa-Aesar), benzene (99%, Aldrich), and 1-hexene (99+%, Aldrich) used in the experiments presented here were purified by several freeze−pump−thaw cycles before introduction into the vacuum chamber, and their

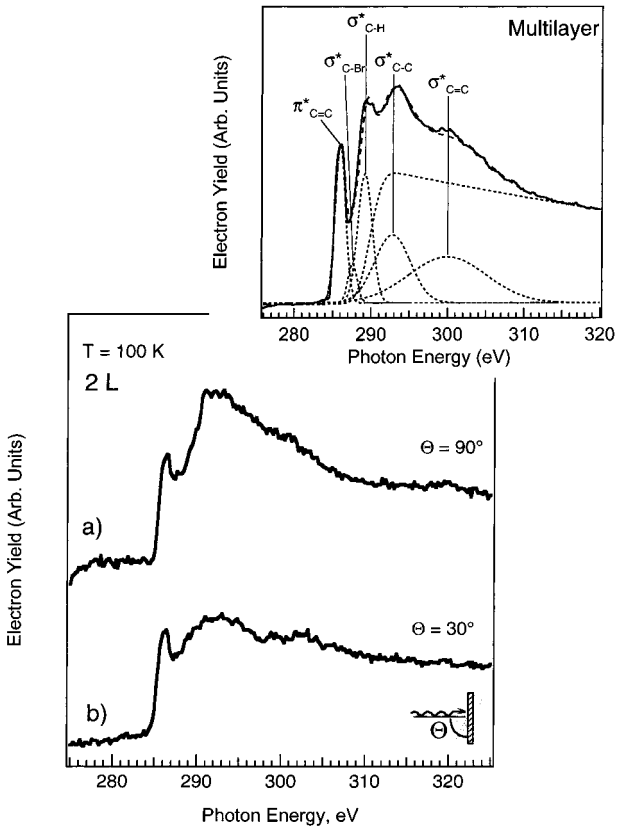

Figure 1. NEXAFS studies of 2 L of 6-bromo-1-hexene on a Cu_3Pt-(111) surface at 100 K at (a) normal and (b) glancing incidence of the photon beam. The inset shows the NEXAFS spectra of the multilayer of 6-bromo-1-hexene with assigned transitions.

purity was confirmed in situ by mass spectrometry. Argon (Matheson) was used without additional purification. All exposures are reported in Langmuirs, where 1 Langmuir is 10^{-6} Torr·s. The exposures are reported without correction of the ion gauge reading for different ion sensitivity.

Results

This section will first present the results of NEXAFS studies of 6-bromo-1-hexene on a $Cu_3Pt(111)$ surface. On the basis of these results, two main adsorption regimes will be defined, and further, each of these regimes will be analyzed in detail by TPR/D.

NEXAFS Studies of 6-Bromo-1-hexene on a $Cu_3Pt(111)$ Surface. Figure 1 presents the NEXAFS measurements of a low exposure of 6-bromo-1-hexene on a $Cu_3Pt(111)$ surface. As it will be shown below, this corresponds to ca. 25% of the exposure required for molecular desorption of 6-bromo-1-hexene from the multilayer to commence. The spectra were recorded at 100 K at normal and glancing incidence of the incoming photon beam. All the transitions corresponding to the molecular 6-bromo-1-hexene are observed in these submonolayer spectra when compared to the multilayer spectrum of this compound shown in the inset to Figure 1. Since the σ^*_{C-Br} transition is observed between the more intense $\pi^*_{C=C}$ and σ^*_{C-H} transitions, assessment of the σ^*_{C-Br} transition is given only approximately and cannot serve as a reliable benchmark to follow its temperature dependence. Although the σ^*_{C-Br} transition is not easily observed, the $\pi^*_{C=C}$ transition gives quite reliable information. The analysis of the NEXAFS spectra shown in Figure 1 suggests that σ^*_{C-C} features exhibit a significant angular dependence. Specifically, these features are much less intense at a glancing

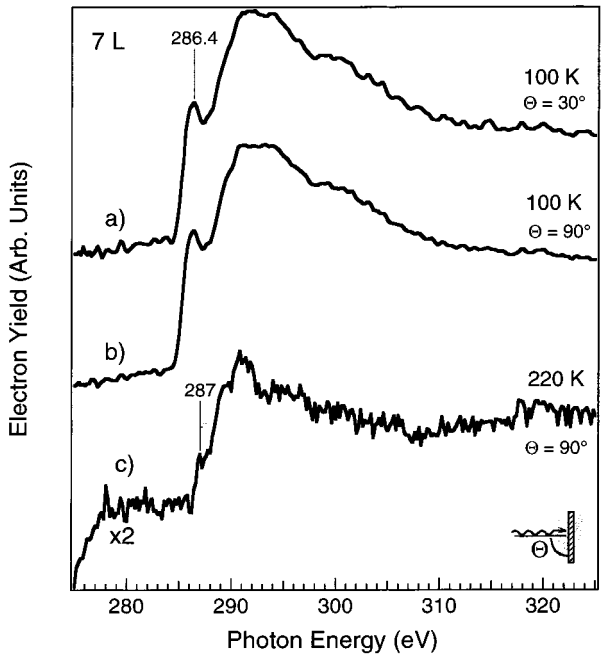

Figure 2. NEXAFS studies of 7 L of 6-bromo-1-hexene on a Cu_3Pt-(111) surface. (a) Glancing incidence of the photon beam, $T = 100$ K. (b) Normal incidence of the photon beam, $T = 100$ K. (c) Normal incidence of the photon beam; the surface was briefly annealed to 300 K after dosing 7 L of 6-bromo-1-hexene and then cooled back to 100 K.

incidence of the photon beam, implying that the carbon−carbon bonds of the molecule are located nearly parallel to the surface. The average angle between the carbon−carbon bonds and the (111) surface can be determined by following the procedure described in ref 77. This angle is approximately 30−35° but large error bars should be placed on this estimate, especially on its lower end, because of the nature of the σ^* transitions and not very high reliability of the procedure for determining the exact intensity of NEXAFS transitions above C K-edge. Interestingly enough, the $\pi^*_{C=C}$ transition does not exhibit any noticeable angular dependence. According to Stöhr,[77] this behavior implies two possible scenarios: (1) C═C bonds are randomly oriented on the surface or (2) the angle between the double bond and the surface is close to the magic angle (54.7°). Both of these explanations suggest that at least a significant portion of double bonds in the surface species at 100 K is not located parallel to the surface. The significance of this observation will be explained in the Discussion section. Plots a and b in Figure 2 show that when the exposure of 6-bromo-1-hexene is increased to 7 L (close to the onset of molecular desorption at the multilayer temperature), no noticeable difference between the spectra taken at normal and glancing incidence of the incoming photon beam is observed. This suggests a random distribution of molecular orientations within this layer.[77] Spectrum 2c will be discussed below.

TPR/D and AES Studies of 6-Bromo-1-hexene on a Cu_3Pt-(111) Surface. (*a) Low-Exposure Regime.* The low-exposure regime is defined here as the adsorption conditions at which the 6-bromo-1-hexene molecules can be arranged on a Cu_3Pt-(111) surface with their C−C bonds approximately parallel to the surface as was described in a previous section. Up to an exposure of 1.5 L, the only hydrocarbon product desorbing from the surface was benzene. It was accompanied by two hydrogen desorption features, 295 and 400 K, presented later in Figure 6, similar to the results of studies of 1-hexene dehydrocyclization.[61,62] No carbon detectable by AES remained on the surface

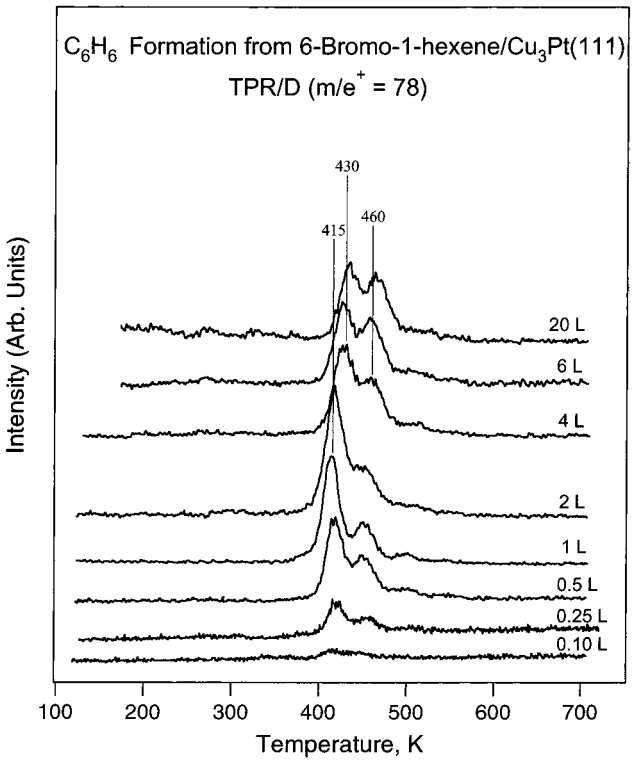

Figure 3. Coverage-dependent TPR/D studies of 6-bromo-1-hexene on a $Cu_3Pt(111)$ surface tracing $m/e^+ = 78$ (benzene formation).

after thermal desorption was complete. Figure 3 shows the results of tracing $m/e^+ = 78$ (molecular mass of benzene) as a function of 6-bromo-1-hexene exposure. The fact that the desorbing entity is benzene was proven by comparing the traces of $m/e^+ = 39$, 50, 52, and 78 to the literature mass spectrum of benzene[78] and by the absence of any other desorption fragments with m/e^+ higher than 78. The two benzene desorption features occur at much higher temperatures than that for benzene molecular desorption[61,62] and the integrated area of the TPR/D peaks reaches a plateau at 1.5 L. Upon further increase of the exposure of 6-bromo-1-hexene, the area of the peaks remains practically unchanged but the kinetics of benzene evolution becomes slightly different. The peak at 415 K shifts up to 430 K and decreases in size. At the same time the temperature of the other desorption peak remains close to 460 K, but the size of this feature increases while the integrated TPR/D area remains constant. The Discussion section will approach this behavior in more detail.

As the exposure of 6-bromo-1-hexene was increased from 1.5 to 3 L, the surface species decomposed and was followed by AES. The ratio of the AES carbon peak at 272 eV to the copper AES signature at 920 eV increases linearly up to the exposure of 3.5 L and then remains unchanged. During this process the only products released into the gas phase were benzene (as described above) and hydrogen. No other hydrocarbon evolution was observed by mass spectrometry. This wraps up the low-coverage behavior of 6-bromo-1-hexene on a $Cu_3Pt(111)$ surface.

(b) High-Exposure Regime. Different behavior of 6-bromo-1-hexene on a $Cu_3Pt(111)$ surface at exposures between 3 and 8.5 L can be explained by the lack of available surface space, effectively blocked by the preceding surface reactions and their products, as will be discussed below.

Figure 4 presents the TPR/D studies of evolution of 1-hexene from a $Cu_3Pt(111)$ surface covered with 6-bromo-1-hexene. 1-Hexene formation is not observed at exposures below 3 L.

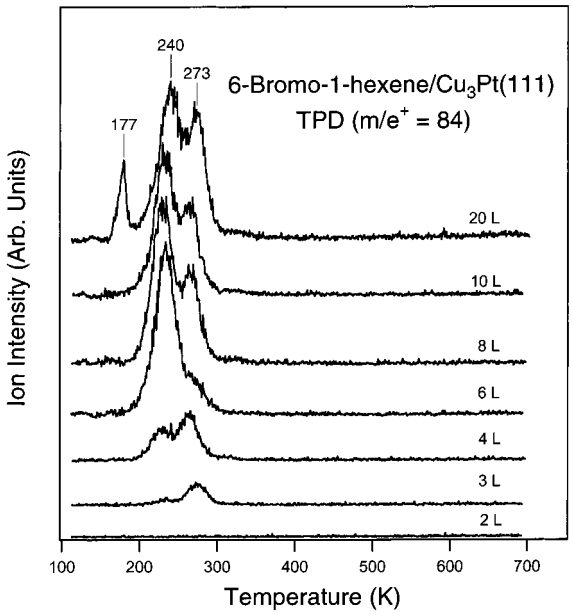

Figure 4. Coverage-dependent TPR/D studies of 6-bromo-1-hexene on a $Cu_3Pt(111)$ surface tracing $m/e^+ = 84$ (1-hexene formation).

A small TPR/D feature is observed at 273 K for exposure of 3 L. As the exposure of 6-bromo-1-hexene is increased, another thermal desorption feature becomes significant for $m/e^+ = 84$ as shown in Figure 4. The integrated area of these two features increases linearly up to the 6 L exposure of 6-bromo-1-hexene. The relative intensities of traces of $m/e^+ = 27$, 39, 55, and 69 collected for several exposures of 6-bromo-1-hexene were compared to the literature data[78] and to the mass spectrum of 1-hexene collected during the back filling of the UHV chamber with 1×10^{-6} Torr of 1-hexene to prove that the desorbing molecule is 1-hexene. The shape of the desorption features depends on the 6-bromo-1-hexene exposure as the higher temperature peak emerges at lower coverages and the lower temperature peak becomes predominant at 6 L. The peak at 177 K observed for the exposure of 20 L in Figure 4 is a cracking pattern resulting from the molecular desorption of unreacted 6-bromo-1-hexene from the multilayer. Valuable information about the mechanism of 1-hexene evolution on a $Cu_3Pt(111)$ surface exposed to 6-bromo-1-hexene can be obtained from Figure 2c. When the surface is briefly annealed to 300 K, most of the surface species responsible for the formation of benzene and surface decomposition should still be on the surface. The peak at 286.4 eV marked in Figure 2a shifts to higher energy and decreases in height (with respect to C K-edge), which is consistent with rehybridization of double bonds of the surface species shown for 1-hexene on the same surface.[61,62] The height of the carbon K-edge corresponding to 7 L of 6-bromo-1-hexene dosed onto the $Cu_3Pt(111)$ surface at 100 K decreases after annealing to 300 K, which can be understood by taking into account the desorption of 6-bromo-1-hexene from the monolayer and the desorption of 1-hexene formed by hydrogenation pathway. This is consistent with thermal desorption experiments.

Figure 5 shows the desorption of 6-bromo-1-hexene from the $Cu_3Pt(111)$ surface as a function of exposure. When molecular $m/e^+ = 162$ is followed by the mass spectrometer as a function of the surface temperature, a desorption feature at 220 K is observed at exposures above 6 L. The area of this feature increases linearly until approximately 8.5 L. At higher exposures multilayer desorption of 6-bromo-1-hexene commences at 177 K. The overall integrated area of the $m/e^+ = 162$ TPR/D features produces a straight line when plotted versus exposure, suggesting

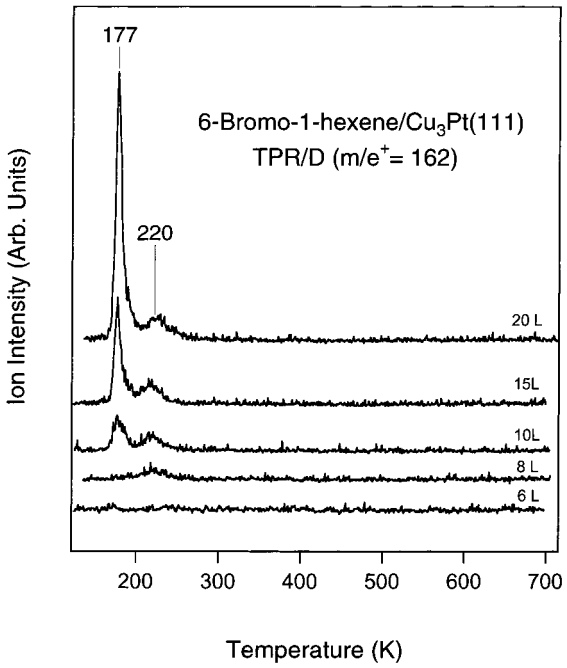

Figure 5. Coverage-dependent TPR/D studies of 6-bromo-1-hexene on a $Cu_3Pt(111)$ surface tracing $m/e^+ = 162$ (6-bromo-1-hexene desorption).

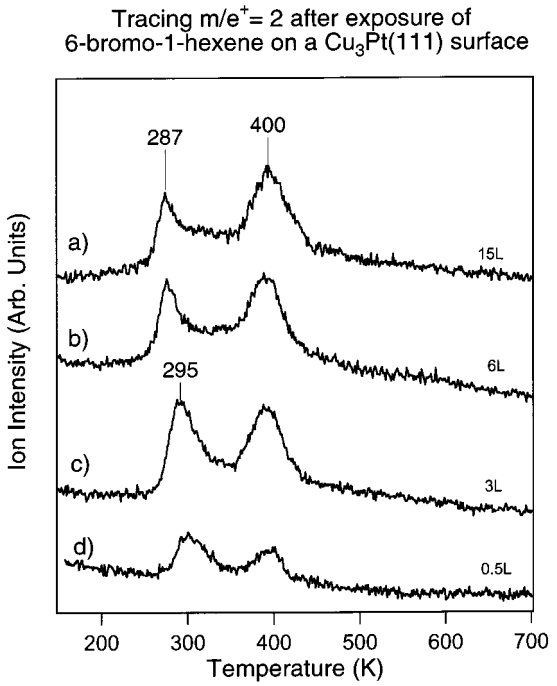

Figure 6. Coverage-dependent TPR/D studies of 6-bromo-1-hexene on a $Cu_3Pt(111)$ surface tracing $m/e^+ = 2$ (evolution of molecular hydrogen).

that above 6 L molecular desorption is the only reaction pathway for 6-bromo-1-hexene on a $Cu_3Pt(111)$ surface. The peak at 220 K corresponds to the molecular desorption from the monolayer, whereas the 177 K feature denotes the multilayer evolution. The AES studies of surface carbon left on the surface after the TPR/D experiment did not show any significant changes for coverages above 6 L. Figure 6 shows the $m/e^+ = 2$ evolution as a function of coverage. Two TPR/D features for hydrogen evolution are present at approximately 295 and 400 K for exposures of 6-bromo-1-hexene below 3 L. This behavior is consistent with the process described in detail in refs 61 and 62. Aromatization or decomposition of the C_6 species arranged approximately parallel to the alloy surface occurs in two steps: (1) dehydrogenation below 300 K, leading to the formation of a surface intermediate that was identified as a hexa-σ-bonded hexatriene for 1-hexene aromatization, and (2) cyclization or decomposition above 400 K, accompanied by the loss of hydrogen atoms in terminal positions. In the case of 6-bromo-1-hexene this mechanism should produce two TPR/D features: at 295 K and at 400 K with the integrated area ratio 3:2 (1.5). The ratio of 1.5 ± 0.3 is observed in all our experiments for hydrogen evolution from exposures of 6-bromo-1-hexene below 3 L. As the exposure of 6-bromo-1-hexene is increased from 3 to 6 L, the high-temperature TPR/D feature shown in Figure 6 does not undergo any significant changes. However, the low-temperature TPR/D feature decreases in size by ~30% and the shape of this feature is consistent with the hydrogenation reaction leading to the formation of 1-hexene shown in Figure 4. For exposures above 6 L, no significant changes in either size or shape of the TPR/D peaks tracing $m/e^+ = 2$ was recorded. Thus, the balance of carbon left on the $Cu_3Pt(111)$ surface after a thermal desorption experiment and the balance of hydrogen leaving the surface during TPR/D remains unchanged for 6-bromo-1-hexene exposures above 6 L, and the molecular desorption of 6-bromo-1-hexene from the monolayer is the only surface process.

Discussion

This section first addresses the NEXAFS studies and analyzes coverage-dependent behavior of 6-bromo-1-hexene on a $Cu_3Pt(111)$ surface. Then thermodynamic implications of this behavior and potential practical uses for aromatization reactions on single-crystal surfaces are outlined.

Coverage-Dependent Behavior of 6-Bromo-1-hexene on a $Cu_3Pt(111)$ Surface. The NEXAFS studies presented in the beginning of the previous section suggest several interesting points. First, the C−C chain is located almost parallel to the surface at low exposures of 6-bromo-1-hexene but at least a significant portion of the adsorbed molecules tilts up as the coverage increases. This behavior is not uncommon for hydrocarbons adsorbed on metal surfaces, but interestingly, the orientation of a carbon−carbon double bond does not seem to depend on the coverage significantly. Previous studies of unsaturated hydrocarbons on the $Cu_3Pt(111)$ surface suggest that the C═C is the most reactive entity in the hydrocarbon structure.[61,62] The double bond is always almost parallel to the surface and it rehybridizes at low temperatures. It was reported to completely rehybridize for 1-hexene on a $Cu_3Pt(111)$ surface at 150 K.[61,62] So why does not the rehybridization or at least a preferential orientation happen for 6-bromo-1-hexene? Here is where the bifunctionality of this compound plays a significant role. It was shown for various halohydrocarbons on transition metal surfaces that halogen-containing hydrocarbons, especially at high coverages, are adsorbed with their C−Hal bond pointed toward the surface.[79,80] The angle between the C−Hal bond and the single-crystal surface depends on many parameters including the nature of the halogen substituent, surface coverage, the structure of the alkyl chain, and the reactivity of the surface; however, in most cases the "heavy" halogen end seems to point toward the surface. In the case of 6-bromo-1-hexene this interaction overwhelms the possibility of interaction of the double bond with the surface even at low coverages. Thus, we do not see any significant rehybridization or angular dependence for the $\sigma^*_{C=C}$ transition in 6-bromo-1-hexene adsorbed on $Cu_3Pt(111)$ at 100 K. Of course, as was noted in the description of

the NEXAFS results, the C−Br bond of 6-bromo-1-hexene is difficult to follow by NEXAFS; however, our studies of the adsorption of other alkyl halides suggest similar behavior and confirm the generality of preferential C−Br adsorption configuration.[81] It should be noted that even though the carbon−carbon double bond does not seem to show any preferential orientation, the nature of the adsorbed species implies that the average *carbon−carbon single bond* may be located at a small angle with respect to the surface at low coverage, which is exactly what coverage-dependent NEXAFS studies of Figures 1 and 2 show.

Although the dissociation of the C−Br bond cannot be accurately followed by the NEXAFS for 6-bromo-1-hexene on $Cu_3Pt(111)$, the studies of other alkyl halides[81] suggest that the temperature of carbon−halogen bond dissociation on this surface should fall between the dissociation temperatures on pure copper and pure platinum. The reported values for alkyl bromides are below 200 K on copper surfaces[82,83] and could be extrapolated to below 250 K on platinum. Only CH_3Br and CH_3CH_2Br were studied on platinum surfaces in detail, and C−Br bond dissociation in these system competes with the dominant molecular desorption (ref 7 and references therein). For these cases the activation energy for C−Br dissociation can be roughly estimated from the molecular desorption data. A crude approximation according to the Redhead method[84] with 10^{13} s^{-1} preexponential factor for the first-order molecular desorption and 10^{11} s^{-1} preexponential factor for the C−Br bond dissociation places the temperature for the C−Br bond dissociation[85,86] somewhere below 250 K. Thus the temperature of C−Br bond dissociation on a $Cu_3Pt(111)$ surface is expected to be close to 200 K.

Figure 7 summarizes the results of TPR/D and AES studies as a function of 6-bromo-1-hexene exposure. It is easily seen that even though the overall chemistry of 6-bromo-1-hexene on a $Cu_3Pt(111)$ surface is quite complicated, each reaction pathway is unique for a given coverage. This behavior allows for calibration of TPR/D peak intensities and AES peak ratios. The only process between 0 and 1.5 L coverage is benzene formation. The only other process between 1.5 and 3 L dose is decomposition, which allows for calibration of AES intensities with respect to the benzene formation. The sensitivity of the mass spectrometer with respect to benzene evolution below 1.5 L and hexene evolution between 3 and 6 L was calibrated by exposing fixed pressures of both compounds to the mass spectrometer and analyzing the ion gauge sensitivities. The straight line was obtained by adding the evolution of benzene and hexene, by adjusting it for the mass spectrometer sensitivities, and by introducing the amount of carbon left on surface (AES results) for exposures up to 6 L. Thus the balance of the reaction products is kept. Similar manipulations can be done for the molecular desorption of 6-bromo-1-hexene. The UHV setup used in the studies presented here did not allow for quantification of the AES peaks corresponding to the adsorbed bromine.

Having established the two possible regimes for the reactions of 6-bromo-1-hexene with the $Cu_3Pt(111)$ surface [(1), C−C is almost parallel to the surface, and (2) random orientation of the adsorbed species] we will next analyze each of these regimes separately.

The low-coverage regime is characterized by chemistry similar to that of 1-hexene reported previously.[61,62] The main difference is the adsorption arrangement. 1-Hexene has been reported to bind with its double bond parallel to the surface and to rehybridize this double bond at low temperature. In the

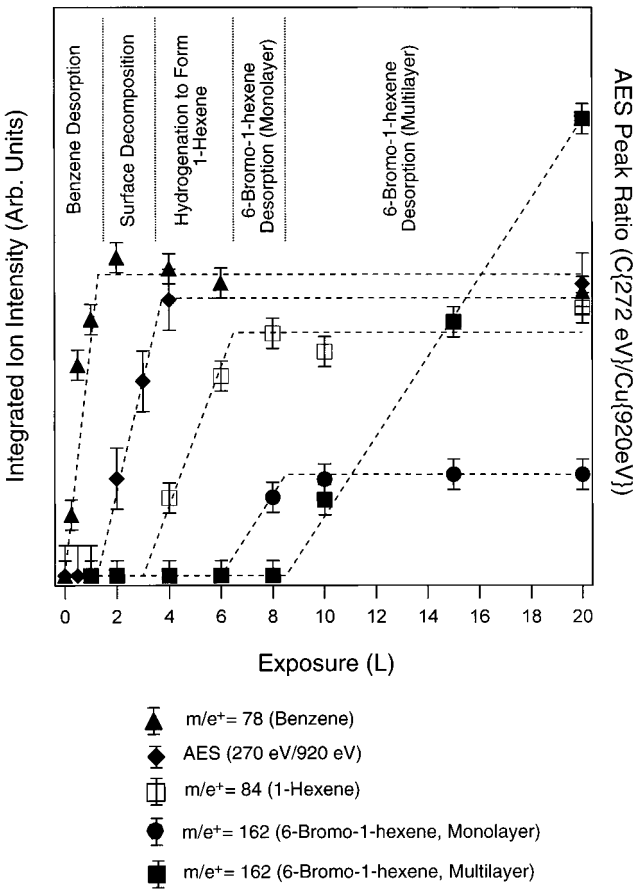

Figure 7. Summary of TPR/D and AES studies of 6-bromo-1-hexene on a $Cu_3Pt(111)$ surface.

case of 6-bromo-1-hexene, we see the bonding to the metal surface through the dissociation of C−Br bond. After the C−Br dissociation occurs, 5-hexenyl species are formed on a surface at low coverage. As the surface temperature is increased, the rehybridized species whose NEXAFS spectrum is presented in Figure 2c is dominant on the surface. The spectral characteristics of this species are similar to those of rehybridized hexatriene, reported to be an intermediate in the aromatization of 1-hexene on $Cu_3Pt(111)$,[61,62] which is depicted in Scheme 1a. The studies presented in references 61 and 62 show that benzene can be formed even from *trans*-hexenes or *trans*-dienes at low coverages, which suggests that the isomerization with respect to the double bond can take place if nearby surface sites are available. At the same time, a high percentage of decomposition was reported for these trans compounds.[61,62] In the case of 6-bromo-1-hexene, the mechanism governing benzene formation as opposed to the decomposition seems to be different. When the double bond is rehybridized at low exposures, the dissociation of the C−Br bond produces surface species that selectively convert to benzene as shown in Scheme 1a. However, as surface coverage is increased, the number of surface sites available for aromatization process decreases. Thus, the dissociation of C−Br at exposures between 1.5 and 3 L produces surface species (probably rehybridized hexatrienes in a conformation shown in Scheme 1b) that are strongly bound to the alloy surface in a configuration from which it is impossible to produce benzene. These surface species decompose upon temperature-programmed reaction. Although the temperature range for benzene evolution from 6-bromo-1-hexene and 1-hexene on a $Cu_3Pt(111)$ surface is similar, the kinetics of benzene evolution is somewhat different. The benzene formation from 6-bromo-1-hexene occurs

SCHEME 1

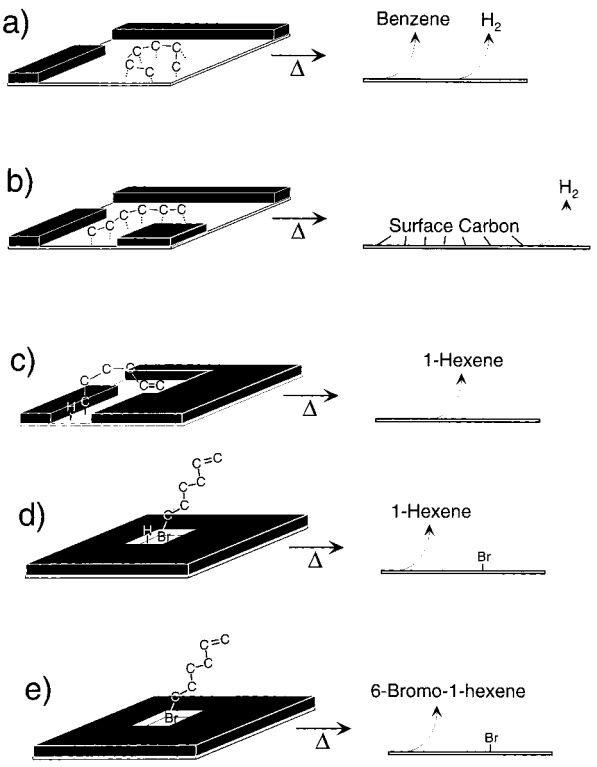

at two temperatures, 430 and 460 K, whereas the temperature of the single feature in the TPR/D spectrum for 1-hexene is 405 K.[61,62] It is likely that the presence of bromine atoms bound to the alloy surface is the reason for this small discrepancy. Similar kinetic behavior was reported for iodoalkanes on copper surfaces.[87,88]

The high-coverage behavior of 6-bromo-1-hexene on a $Cu_3Pt(111)$ surface is even more interesting. As suggested in Scheme 1c−e, when surface coverage is raised above 3 L, surface space is already so limited that a flat configuration amenable for aromatization or surface decomposition cannot be attained. Thus the surface coverage of 6-bromo-1-hexene self-governs the following surface transformations. As molecular desorption of 6-bromo-1-hexene from a monolayer competes with C−Br bond dissociation, three possible reactions involving hexenyl species produced by this dissociation may take place. Once formed, a 5-hexenyl radical can bind to the alloy surface as shown in Scheme 1c or react with any available surface species. The formation of 1,11-dodecadiene could be the result of a coupling of 5-hexenyl radical with another 5-hexenyl radical. The product of this transformation was not observed by mass spectrometry in the studies presented here. Neither were 5-hexenyl radicals ejected from the surface or any products with more than six carbon atoms that could result from reaction of 5-hexenyl radical with the products of decomposition found for exposures of 6-bromo-1-hexene between 1.5 and 3 L. The carbon content checked by AES after thermal desorption experiments did not change for the exposures above 3 L. The only reaction induced by the high coverages of 6-bromo-1-hexene was the hydrogenation of 5-hexenyl species to produce 1-hexene. The evolution of 1-hexene from the $Cu_3Pt(111)$ surface recorded by TPR/D experiments follows the kinetics of simple 1-hexene desorption rather than that of the surface hydrogenation reaction as is proven by the experiment presented in Figure 8. A clean $Cu_3Pt(111)$ surface was exposed to 3 L of 6-bromo-1-hexene, and then an extra 1 L of 1-hexene was deposited. As demonstrated above, 3 L of 6-bromo-1-hexene

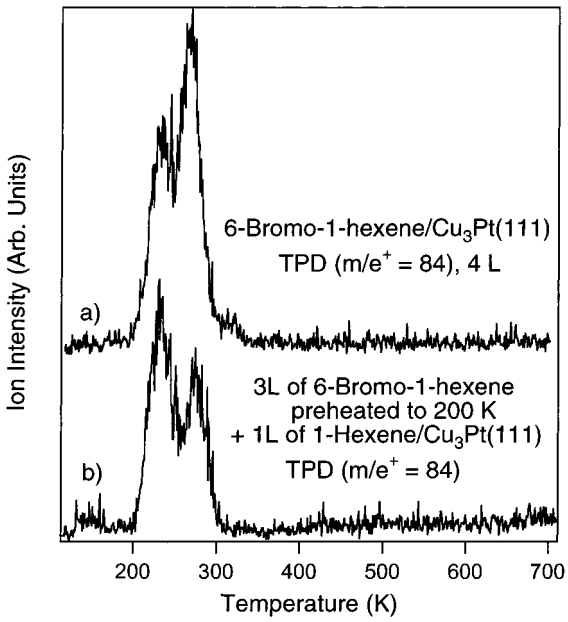

Figure 8. Comparison of TPR/D traces following $m/e^+ = 84$ for (a) evolution of 4 L of 6-bromo-1-hexene on a $Cu_3Pt(111)$ surface and (b) evolution of 1 L of 1-hexene dosed on top of 3 L of 6-bromo-1-hexene on a $Cu_3Pt(111)$ surface.

transforms into either benzene or into the decomposition products. No 1-hexene should be formed at this exposure. The TPD evolution of 1-hexene adsorbed on a surface in such a manner, shown in Figure 8b, looks almost identical to the evolution of 1-hexene when a clean $Cu_3Pt(111)$ surface is exposed to 4 L of 6-bromo-1-hexene. A small difference in exposure can be explained by different ion gauge sensitivities toward 1-hexene and 6-bromo-1-hexene. This experiment proves that the evolution of 1-hexene from a $Cu_3Pt(111)$ surface covered with 6-bromo-1-hexene reflects 1-hexene desorption kinetics rather than its formation, which should happen concurrently with the C−Br bond dissociation. The two possibilities outlined in Scheme 1c,d cannot be distinguished on the basis of the studies presented here. However, since molecular desorption of 6-bromo-1-hexene from a monolayer is observed even with the excess of hydrogen available on a surface (Scheme 1e), the scenario depicted in Scheme 1d is unlikely. Finally, it should be noted that the double bonds of the species left on a $Cu_3Pt(111)$ surface after a high exposure of 6-bromo-1-hexene is annealed to 300 K seem to be rehybridized according to the NEXAFS data presented in Figure 2c. The fact that resulting hexene molecules do not aromatize is indicative of an arrangement of the alkyl chain in which, even if the terminal double bond is rehybridized, the rest of the alkyl chain is not in contact with the $Cu_3Pt(111)$ surface because of the restricted geometry dictated by other surface processes.

Thermodynamic Implications for Dissociation and Hydrogenation Reactions on $Cu_3Pt(111)$. The thermodynamics of the processes described above will be difficult to follow because of the lack of experimental data for these processes when they occur on a surface of a bimetallic alloy. Nevertheless, several important points can be emphasized on the basis of the studies presented here.

The process that precedes the interesting chemistry observed for 6-bromo-1-hexene on a $Cu_3Pt(111)$ surface is C−Br dissociation. The thermodynamics for carbon−halogen bond dissociation was considered in detail for a reaction on pure copper[82,89−91] and pure platinum.[80,92] Our studies of cyclohexyl halides on a $Cu_3Pt(111)$ surface[81] suggest that the dissociation

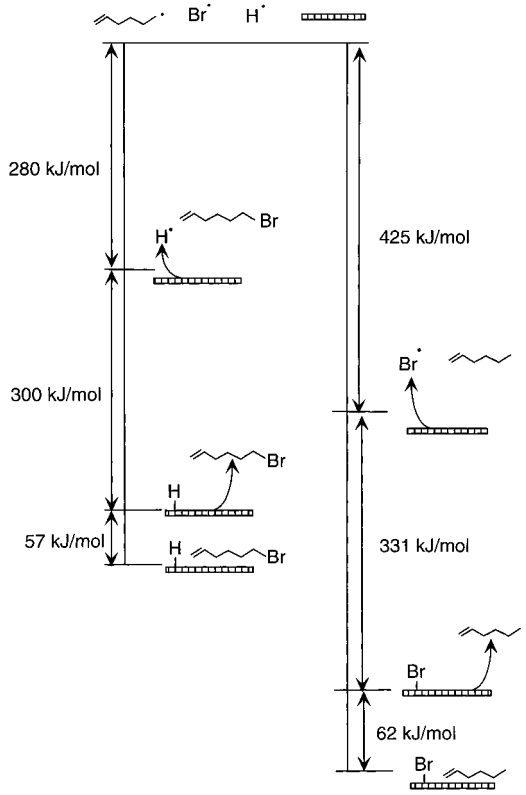

Figure 9. Thermochemical cycle for 6-bromo-1-hexene hydrogenation on a $Cu_3Pt(111)$ surface.

temperatures for alkyl halides on this surface lie between the dissociation temperatures for the same compounds on Cu(111) and Pt(111). As discussed above, C−Br dissociation on a $Cu_3Pt(111)$ surface occurs around 200 K. The activation energy associated with the C−Br dissociation can be estimated by the Redhead method[84] with the preexponential factor of 10^{11} s^{-1}.[91] The activation energy found by this approach is ∼44 kJ/mol. The main mechanism for C−Hal bond dissociation on Cu(111) was proposed to involve thermally activated electron transfer from copper to alkyl halide.[91] The dissociation of methyl iodide was analyzed in detail by this approach and the activation energy for a dissociation process was found to be consistent with the suggested mechanism.[91]

A thermochemical cycle for analysis of the hydrogenation process is presented in Figure 9. Some of the numbers for this analysis can be obtained from our measurements; others can be estimated from the literature data. The desorption barrier for the monolayer of 6-bromo-1-hexene on a $Cu_3Pt(111)$ surface can be estimated from a TPR/D feature at 220 K (see Figure 5). The first-order approximation[84] with a preexponential factor of 10^{13} s^{-1} [93] yields a desorption activation energy of 57 kJ/mol. The energies of the Cu−H bond and the Pt−H bond in diatomic molecules are 278 and 335 kJ/mol, respectively.[94] The average value of approximately 300 kJ/mol will be sufficient for our discussion. The energy of the C−Br bond in a gas phase is approximately 280 kJ/mol.[94] The energy of a metal−bromine bond is estimated at 331 kJ/mol from the gas-phase bond energy in Cu−Br.[94] This number may be slightly different on a $Cu_3Pt(111)$ surface, but the experimental data suggest that the strength of the halogen−metal bond is similar on copper and platinum.[80,95] The energy of the C−H bond can be obtained from the gas-phase values at approximately 425 kJ/mol. Finally, the desorption barrier for 1-hexene is calculated from our thermal desorption data and yields 62 kJ/mol if the Redhead method[84] with a 10^{13} s^{-1} preexponential factor is used for the 240 K TPR/D feature in Figure 4. Thus, the overall hydrogenation reaction is exothermic by 181 kJ/mol.

Conclusions

The chemistry of 6-bromo-1-hexene on a $Cu_3Pt(111)$ surface was studied by NEXAFS, TPR/D, and AES. It was found that the reactions of this compound show strong coverage dependence on the surface of the bimetallic alloy. Two distinctly different coverage ranges are determined by NEXAFS measurements: low coverage, with C−C bonds of the alkyl chain arranged approximately parallel to the single-crystal surface, and high coverage, with a random distribution of the angles between C−C bonds and the alloy surface. Dehydrocyclization is the only process observed at very low coverages. As the coverage of 6-bromo-1-hexene is increased, decomposition becomes noticeable as long as the alkyl chain is approximately parallel to the surface. When the surface of the alloy becomes crowded, two other chemical reactions dominate the transformations of 6-bromo-1-hexene on a $Cu_3Pt(111)$ surface. If hydrogenation is kinetically allowed, it dominates at the exposures between 3 and 6 L. Upon further increase of the surface coverage of the adsorbed 6-bromo-1-hexene, molecular desorption of this compound commences from the monolayer up to the exposure of 8.5 L, when zero-order desorption from a multilayer becomes dominant.

Acknowledgment. We acknowledge the help of Professor Jingguang G. Chen (Materials Science Department, University of Delaware) for his assistance with the NEXAFS experiments. A.V.T. thanks the Chemistry Department of Columbia University for the donation of some of the equipment used to prepare this publication.

References and Notes

(1) Ertl, G. *Catal. Rev.* **1980**, *21*, 201−223.
(2) Bent, B. E.; Somorjai, D. A. *Adv. Colloid Interface Sci.* **1989**, *29*, 223.
(3) Canning, E. L.; Madix, R. J. *J. Phys. Chem.* **1984**, *88*, 2437−2446.
(4) Muetterties, E. L. *Chem. Soc. Rev.* **1982**, *11*, 283−320.
(5) Sheppard, N. *Annu. Rev. Phys. Chem.* **1988**, *39*, 589−644.
(6) Fisher, G. B. In *Characterization and Metal Catalysis*; Fisher, G. B., Ed.; Chemical Institute of Canada: Ottawa, Canada, 1988; Vol. 3.
(7) Bent, B. E. *Chem. Rev.* **1996**, *96*, 1361−1390.
(8) Zaera, F. *Acc. Chem. Res.* **1992**, *25*, 260−265.
(9) Zaera, F. *Chem. Rev.* **1995**, *95*, 2651−2693.
(10) White, J. M. *Langmuir* **1994**, *10*, 3946−3954.
(11) Weldon, M. K.; Friend, C. M. *Chem. Rev.* **1996**, *96*, 1391−1411.
(12) Goodman, D. W. *Chem. Rev.* **1995**, *95*, 523−536.
(13) Barteau, M. A. *Chem. Rev.* **1996**, *96*, 1413−1430.
(14) Somorjai, G. A. *Chem. Rev.* **1996**, *96*, 1223−1235.
(15) Gates, B. C. *Chem. Rev.* **1995**, *95*, 511−522.
(16) Xu, C.; Tsai, Y.-L.; Koel, B. E. *J. Phys. Chem.* **1994**, *98*, 585−593.
(17) Xu, C.; Koel, B. E. *Surf. Sci.* **1994**, *304*, 249−266.
(18) Park, Y. K.; Ribeiro, F. H.; Somorjai, G. A. *J. Catal.* **1998**, *178*, 66−75.
(19) Sachtler, J. W. A.; Van Hove, M. A.; Bibérian, J. P.; Somorjai, G. A. *Phys. Rev. Lett.* **1980**, *45*, 1601.
(20) Sachtler, J. W. A.; Somorjai, G. A. *J. Catal.* **1983**, *81*, 77.
(21) Sachtler, J. W. A.; Somorjai, G. A. *J. Catal.* **1984**, *89*, 35−43.
(22) Xu, C.; Peck, J. W.; Koel, B. E. *J. Am. Chem. Soc.* **1993**, *115*, 751−755.
(23) Campbell, C. T.; Campbell, J. M.; Dalton, P. J.; Henn, F. C.; Rodriguez, J. A.; Seimanidis, S. G. *J. Phys. Chem.* **1989**, *93*, 806−814.
(24) Campbell, J. M.; Siemanides, S.; Campbell, C. T. *J. Phys. Chem.* **1989**, *93*, 815−826.
(25) Rodriguez, J. A.; Campbell, C. T. *J. Phys. Chem.* **1989**, *93*, 826−835.
(26) Henn, F. C.; Dalton, P. J.; Campbell, C. T. *J. Phys. Chem.* **1989**, *93*, 836−846.
(27) Newton, M. A.; Campbell, C. T. *Z. Phys. Chem.* **1997**, *198*, 169−187.

(28) Sinfelt, J. H. *Adv. Catal.* **1973**, *23*, 91−119.
(29) Sachtler, W. M. H.; vanSanten, R. A. *Adv. Catal.* **1977**, *26*, 69−119.
(30) Yermakov, Y. I.; Kuznetsov, B. N.; Zakharov, V. A. *Catalysis by Supported Complexes*; Elsevier: Amsterdam, 1981; Vol. 8.
(31) Carter, J. L.; McVicker, G. B.; Weissman, W.; Kmak, W. S.; Sinfelt, J. H. *Appl. Catal.* **1982**, *3*, 327−346.
(32) Botman, M. J. P.; deVreugd, K.; Zandbergen, H. W.; deBlock, R.; Ponec, V. *J. Catal.* **1989**, *116*, 467−479.
(33) Rodriguez, J. A. *Surf. Sci. Rep.* **1996**, *24*, 223−287.
(34) Peden, C. H. F.; Goodman, D. W. *J. Catal.* **1987**, *104*, 347−358.
(35) Dautzenberg, F. M.; Helle, J. N.; Biloen, P.; Sachtler, W. M. H. *J. Catal.* **1980**, *63*, 119−128.
(36) de Jongste, H. C.; Kuijers, F. J.; Ponec, V. *Prepr. Catal., Proc. Int. Symp.* **1975**, **1976**, 207.
(37) de Jongste, H. C.; Kuijers, F. J.; Ponec, V. *Proc. Int. Congr. Catal. 6th*, **1976**, **1977**, *2*, 915−926.
(38) de Jongste, H. C.; Ponec, V. *J. Catal.* **1980**, *63*, 389−394.
(39) de Jongste, H. C.; Ponec, V.; Gault, F. G. *J. Catal.* **1980**, *63*, 395−403.
(40) Vadlamannati, L. S.; Kovalchuk, V. I.; D'Itri, J. L. *Catal. Lett.* **1999**, *58*, 173−178.
(41) Ginatempo, B.; Guo, G. Y.; Temmerman, W. M.; Staunton, J. B.; Durham, P. J. *Phys. Rev. B* **1990**, *42*, 2761−2767.
(42) Miura, S.; Mitsui, K.; Tanaka, Y.; Mishima, Y.; Suzuki, T. *Philos. Mag. A* **1992**, *65*, 737−747.
(43) Kuwano, N.; Matsumoto, A.; Kajiwara, K.; Oki, K. *Mater. Trans., JIM* **1993**, *34*, 1163−1168.
(44) Shen, Y. G.; O'Connor, D. J.; MacDonald, R. J.; Wandelt, K. *Solid State Commun.* **1995**, *96*, 557−562.
(45) Shen, Y. G.; O'Connor, D. J.; MacDonald, R. J. *J. Phys.: Condens. Matter* **1997**, *9*, 8345−8358.
(46) Shen, Y. G.; O'Connor, D. J.; Wandelt, K. *Surf. Sci.* **1998**, *410*, 1−14.
(47) Shen, Y. G.; O'Connor, D. J.; Wandelt, K. *Surf. Sci.* **1998**, *406*, 23−31.
(48) Mitsui, K.; Takahashi, M.; Takezawa, T. *Philos. Mag. Lett.* **1998**, *77*, 49−57.
(49) Matsumoto, A.; Matsuno, K.; Oki, K. *J. Electron Microsc.* **1996**, *45*, 442.
(50) Hammer, B.; Nørskov, J. K. *Surf. Sci.* **1995**, *343*, 211−220.
(51) Schneider, U.; Castro, G. R.; Busse, H.; Janssens, T.; Wesemann, J.; Wandelt, K. *Surf. Sci.* **1992**, *269/270*, 316−320.
(52) Linke, R.; Schneider, U.; Busse, H.; Becker, C.; Shröder, U.; Castro, G. R.; Wandelt, K. *Surf. Sci.* **1994**, *307/309*, 407−411.
(53) Boo, J. B.; Lee, S. B.; Linke, R.; Becker, C.; Shröder, U.; Wandelt, K. *J. Korean Phys. Soc.* **1999**, *35*, S582−S587.
(54) Schneider, U.; Busse, H.; Linke, R.; Castro, G. R.; Wandelt, K. *J. Vac. Sci. Technol. A* **1994**, *12*, 2069−2073.
(55) Becker, C.; Shröder, U.; Castro, G. R.; Schneider, U.; Busse, H.; Linke, R.; Wandelt, K. *Surf. Sci.* **1994**, *307/309*, 412−415.
(56) Castro, G. R.; Doyen, G. *Surf. Sci.* **1994**, *307/309*, 384−389.
(57) Castro, G. R.; Schneider, U.; Busse, H.; Janssens, T.; Wandelt, K. *Surf. Sci.* **1992**, *269−270*, 321−325.
(58) Becker, C.; Pelster, T.; Tanemura, M.; Breitbach, J.; Wandelt, K. *Surf. Sci.* **1999**, *428*, 403−407.
(59) Holzwarth, A.; Loboda-Cackovic, J.; Block, J. H.; Christmann, K. *Z. Phys. Chem.* **1996**, *196*, 55−72.
(60) Shen, Y. G.; O'Connor, D. J.; MacDonald, R. J. *Aust. J. Phys.* **1996**, *49*, 689−704.
(61) Teplyakov, A. V.; Bent, B. E. *J. Phys. Chem. B* **1997**, *101*, 9052−9059.
(62) Teplyakov, A. V.; Gurevich, A. B.; Garland, E. R.; Bent, B. E. *Langmuir* **1998**, *14*, 1337−1344.
(63) Lin, J. L.; Bent, B. E. *J. Am. Chem. Soc.* **1993**, *115*, 6943−6950.
(64) Jaramillo, D. M.; Hunka, D. E.; Land, D. P. *Surf. Sci.* **2000**, *445*, 23−41.
(65) Khairutdinov, R. F. *Prog. Reaction Kinetics* **1996**, *21*, 1−68.
(66) Tachiya, M. In *Kinetics of Non Homogeneous Processes*; Tachiya, M., Ed.; Wiley: New York, 1987; p 575.
(67) Ramamurthy, V. In *Photochemistry in Organized and Constrained Media*; Ramamurthy, V., Ed.; VCH Publishers: New York, 1991; p 429.
(68) Almgren, M. In *Kinetics and Catalysis in Microheterogeneous Systems*; Almgren, M., Ed.; Marcel Dekker: New York, 1991; p 63.
(69) Ediger, M. D.; Fayer, M. D. *Macromolecules* **1983**, *16*, 13.
(70) Möbius, D. In *Kinetics of Non Homogeneous Processes*; Möbius, D., Ed.; Wiley: New York, 1987; p 533.
(71) Klafter, J.; Drake, J. M. *Molecular Dynamics in Restricted Geometries*; Klafter, J., Drake, J. M., Eds.; Wiley: New York, 1989.
(72) Drake, J. M.; Levitz, P.; Turro, N. J.; Nitsche, K. S.; Cassidy, K. F. *J. Phys. Chem.* **1988**, *92*, 4680.
(73) Fisher, D. A.; Colbert, J.; Gland, J. L. *Rev. Sci. Instrum.* **1989**, *60*, 1596−1602.
(74) Outka, D. A.; Stöhr, J. *J. Chem. Phys.* **1988**, *86*, 3539−3554.
(75) Shen, Y. G.; O'Connor, D. J.; Wandelt, K.; MacDonald, R. J. *Surf. Sci.* **1995**, *328*, 21−31.
(76) Shen, Y. G.; O'Connor, D. J.; Wandelt, K.; MacDonald, R. J. *Surf. Sci.* **1995**, *331−333*, 746.
(77) Stöhr, J. *NEXAFS Spectroscopy*; Springer: Berlin, 1996; Vol. 25.
(78) Heller, S. R.; Milne, G. W. A. *EPA/NIH Mass Spectral Data Base*; Heller, S. R., Milne, G. W. A., Eds.; U.S. Government Printing Office: Washington, DC, 1978; Vol. 1.
(79) Zaera, F.; Hoffmann, H.; Griffiths, P. R. *J. Electron Spectrosc. Relat. Phenom.* **1990**, *54/55*, 705−715.
(80) Zaera, F.; Hoffmann, H. *J. Phys. Chem.* **1991**, *95*, 6297−6303.
(81) Mathauser, A. T.; He, H.; Teplyakov, A. V. Submitted to *Surf. Sci.*
(82) Lin, J.-L.; Bent, B. E. *J. Phys. Chem.* **1992**, *96*, 8529−8538.
(83) Lin, J. L.; Teplyakov, A. V.; Bent, B. E. *J. Phys. Chem.* **1996**, *100*, 10721−10731.
(84) Redhead, P. A. *Vacuum* **1962**, *12*, 203.
(85) Henderson, M. A.; Mitchell, G. E.; White, J. M. *Surf. Sci. Lett.* **1987**, *184*, L325.
(86) Zaera, F.; Hoffmann, H.; Griffiths, P. R. *J. Electron Spectrosc. Relat. Phenom.* **1990**, *54/55*, 705.
(87) Paul, A.; Jenks, C. J.; Bent, B. E. *Surf. Sci.* **1992**, *261*, 233−242.
(88) Chiang, C.-M.; Bent, B. E. *Surf. Sci.* **1992**, *279*, 79−88.
(89) Chiang, C.-M.; Bent, B. E. *J. Vac. Sci. Technol. A* **1992**, *10*, 2202−2209.
(90) Chiang, C.-M.; Wentzlaff, T. H.; Bent, B. E. *J. Phys. Chem.* **1992**, *96*, 1836−1848.
(91) Lin, J.-L.; Bent, B. E. *J. Phys. Chem.* **1993**, *97*, 9713−9718.
(92) Zaera, F. *J. Phys. Chem.* **1990**, *94*, 8350−8355.
(93) Teplyakov, A. V.; Bent, B. E. *J. Am. Chem. Soc.* **1995**, *117*, 10076−10087.
(94) *CRC Handbook of Chemistry and Physics*, 81st ed.; Chemical Rubber Co.: Boca Raton, FL, 2000−2001.
(95) Lin, J. L.; Bent, B. E. *J. Am. Chem. Soc.* **1993**, *115*, 2849−2853.